Iridium(I) versus Ruthenium(II). A Computational Study of the Transition Metal Catalyzed Transfer Hydrogenation of Ketones

Jan-Willem Handgraaf,[†] Joost N. H. Reek,[‡] and Evert Jan Meijer*,[†]

Department of Chemical Engineering, University of Amsterdam, Nieuwe Achtergracht 166, 1018 WV Amsterdam, The Netherlands, and Institute of Molecular Chemistry, University of Amsterdam, Nieuwe Achtergracht 166, 1018 WV Amsterdam, The Netherlands

Received February 14, 2003

We present a density functional theory based computational study comparing simplified models for the ruthenium(II)- and iridium(I)-catalyzed transfer hydrogenation of ketones. For the ruthenium compound our results confirm earlier findings that the hydrogenation involves a ruthenium hydride and occurs via a concerted hydrogen transfer mechanism with no direct ruthenium−ketone binding along the reaction path. In contrast, for the iridium compound our calculations suggest that the reaction proceeds via direct hydrogen transfer between simultaneously coordinated ketone and alcohol. We find that for both metal complexes the formation of a very stable metal−alkoxide complex plays an important role. For the ruthenium-catalyzed reaction it constitutes a resting state that does not take an active part in the transfer hydrogenation, while for the iridium-catalyzed reaction it is an important intermediate along the reaction path.

Introduction

One of the most fundamental transformations in synthetic chemistry is the asymmetric reduction of C═O and C═N bonds forming stereospecific centers in molecules.[1] In this field, Noyori et al. initiated significant progress by introducing well-designed chiral ruthenium compounds that catalyze transfer hydrogenation from 2-propanol to pro-chiral ketones with a high enantioselectivity.[2] Subsequently, various other chiral compounds with a ruthenium(II)[2−25] (Ru), rhodium(I)[26−36] (Rh), or iridium(I)[28,32,33,35,37−41] (Ir) catalytic metal center have been designed that shown both a high yield and a high enantioselectivity under relatively mild

* Corresponding author. Fax: +31-20-525-5604. E-mail: ejmeijer@science.uva.nl.
[†] Department of Chemical Engineering.
[‡] Institute of Molecular Chemistry.

(1) Noyori, R. *Asymmetric Catalysis in Organic Synthesis;* Wiley: New York, 1994.
(2) Hashiguchi, S.; Fujii, A.; Takehara, J.; Ikariya, T.; Noyori, R. *J. Am. Chem. Soc.* **1995**, *117*, 7562−7563.
(3) Yang, H.; Alvarez, M.; Lugan, N.; Mathieu, R. *J. Chem. Soc., Chem. Commun.* **1995**, 1721−1722.
(4) Fujii, A.; Hashiguchi, S.; Uematsu, N.; Ikariya, T.; Noyori, R. *J. Am. Chem. Soc.* **1996**, *118*, 2521−2522.
(5) Gao, J.-X.; Ikariya, T.; Noyori, R. *Organometallics* **1996**, *15*, 1087−1089.
(6) Jiang, Q. Z.; Plew, D. V.; Murtuza, S.; Zhang, X. M. *Tetrahedron Lett.* **1996**, *37*, 797−800.
(7) Takehara, J.; Hashiguchi, S.; Fujii, A.; Inoue, S.; Ikariya, T.; Noyori, R. *Chem. Commun.* **1996**, 233−234.
(8) Haack, K.-J.; Hashiguchi, S.; Fujii, A.; Ikariya, T.; Noyori, R. *Angew. Chem., Int. Ed. Engl.* **1997**, *36*, 285−288.
(9) Hashiguchi, S.; Fujii, A.; Haack, K.-J.; Matsumura, K.; Ikariya, T.; Noyori, R. *Angew. Chem., Int. Ed. Engl.* **1997**, *36*, 288−290.
(10) ter Halle, R.; Schulz, E.; Lemaire, M. *Synlett* **1997**, 1257−1258.
(11) Matsumura, K.; Hashiguchi, S.; Ikariya, T.; Noyori, R. *J. Am. Chem. Soc.* **1997**, *119*, 8738−8739.
(12) Noyori, R.; Hashiguchi, S. *Acc. Chem. Res.* **1997**, *30*, 97−102.
(13) Palmer, M.; Walsgrove, T.; Wills, M. *J. Org. Chem.* **1997**, *62*, 5226−5228.
(14) Alonso, D. A.; Guijarro, D.; Pinho, P.; Temme, O.; Andersson, P. G. *J. Org. Chem.* **1998**, *63*, 2749−2751.
(15) Jiang, Y. T.; Jiang, Q. Z.; Zhang, X. M. *J. Am. Chem. Soc.* **1998**, *120*, 3817−3818.
(16) Schwink, L.; Ireland, T.; Püntener, K.; Knochel, P. *Tetrahedron: Asymmetry* **1998**, *9*, 1143−1163.
(17) Aranyos, A.; Csjernyik, G.; Szabó, K. J.; Bäckvall, J.-E. *Chem. Commun.* **1999**, 351−352.
(18) Braunstein, P.; Fryzuk, M. D.; Naud, F.; Rettig, S. J. *J. Chem. Soc., Dalton Trans.* **1999**, 589−594.
(19) Alonso, D. A.; Nordin, S. J. M.; Roth, P.; Tarnai, T.; Andersson, P. G.; Thommen, M.; Pittelkow, U. *J. Org. Chem.* **2000**, *65*, 3116−3122.
(20) Braunstein, P.; Naud, F.; Graiff, C.; Tiripicchio, A. *Chem. Commun.* **2000**, 897−898.
(21) Ohkuma, T.; Ishii, D.; Takeno, H.; Noyori, R. *J. Am. Chem. Soc.* **2000**, *122*, 6510−6511.
(22) Petra, D. G. I.; Reek, J. N. H.; Handgraaf, J.-W.; Meijer, E. J.; Dierkes, P.; Kamer, P. C. J.; Brussee, J.; Schoemaker, H. E.; van Leeuwen, P. W. N. M. *Chem. Eur. J.* **2000**, *6*, 2818−2829.
(23) Quirmbach, M.; Holz, J.; Tararov, V. I.; Börner, A. *Tetrahedron* **2000**, *56*, 775−780.
(24) Braunstein, P.; Naud, F.; Rettig, S. J. *New J. Chem.* **2001**, *25*, 32−39.
(25) Everaere, K.; Mortreux, A.; Bulliard, M.; Brussee, J.; van der Gen, A.; Nowogrocki, G.; Carpentier, J.-F. *Eur. J. Org. Chem.* **2001**, 275−291.
(26) Gamez, P.; Fache, F.; Mangeney, P.; Lemaire, M. *Tetrahedron Lett.* **1993**, *34*, 6897−6898.
(27) Gamez, P.; Fache, F.; Lemaire, M. *Tetrahedron: Asymmetry* **1995**, *6*, 705−718.
(28) Gamez, P.; Dunjic, B.; Lemaire, M. *J. Org. Chem.* **1996**, *61*, 5196−5197.
(29) Nishibayashi, Y.; Singh, J. D.; Arikawa, Y.; Uemura, S.; Hidai, M. *J. Organomet. Chem.* **1997**, *531*, 13−18.
(30) Bernard, M.; Guiral, V.; Delbecq, F.; Fache, F.; Sautet, P.; Lemaire, M. *J. Am. Chem. Soc.* **1998**, *120*, 1441−1446.
(31) de Bellefon, C.; Tanchoux, N. *Tetrahedron: Asymmetry* **1998**, *9*, 3677−3686.
(32) Mashima, K.; Abe, T.; Tani, K. *Chem. Lett.* **1998**, 1199−1200.
(33) Mashima, K.; Abe, T.; Tani, K. *Chem. Lett.* **1998**, 1201−1202.
(34) Mao, J. M.; Baker, D. C. *Org. Lett.* **1999**, *1*, 841−843.
(35) Murata, K.; Ikariya, T. *J. Org. Chem.* **1999**, *64*, 2186−2187.
(36) Polborn, K.; Severin, K. *Eur. J. Inorg. Chem.* **2000**, 1687−1692.
(37) Zassinovich, G.; Bettella, R.; Mestroni, G.; Bresciani-Pahor, N.; Geremia, S.; Randaccio, L. *J. Organomet. Chem.* **1989**, *370*, 187−202.
(38) Müller, D.; Umbricht, G.; Weber, B.; Pfaltz, A. *Helv. Chim. Acta* **1991**, *74*, 232−240.
(39) ter Halle, R.; Bréhéret, A.; Schulz, E.; Pinel, C.; Lemaire, M. *Tetrahedron: Asymmetry* **1997**, *8*, 2101−2108.

10.1021/om030104t CCC: $25.00
Publication on Web 06/17/2003

Scheme 1. Mechanistic Alternatives for Transition Metal Catalyzed Asymmetric Hydrogen Transfer: (I) Concerted Hydrogen Transfer, (II) Migratory Insertion, and (III) Direct Hydrogen Transfer[a]

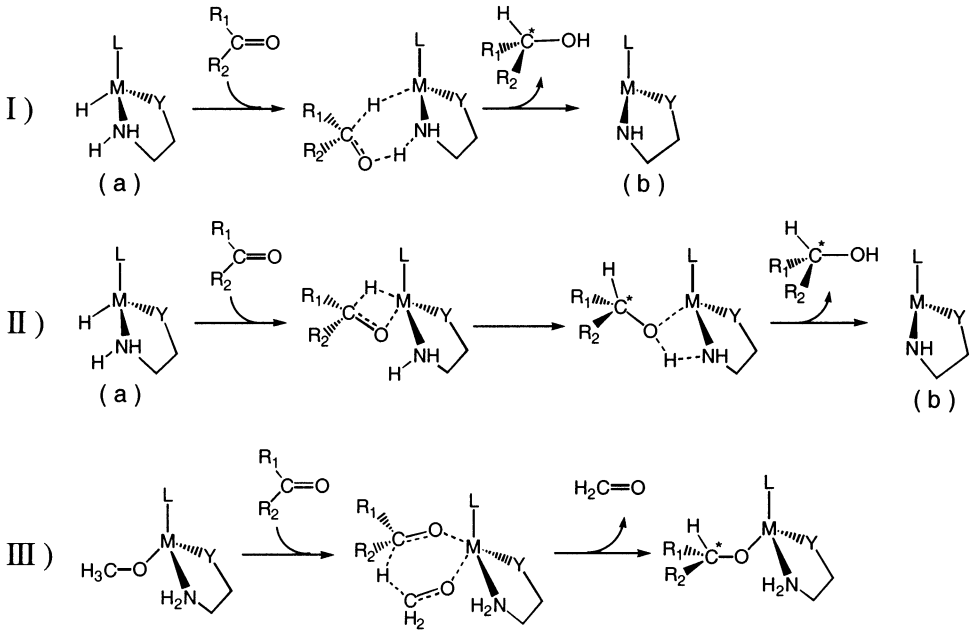

[a] M = transition metal, L = arene or olefin, and Y = nitrogen, oxygen, or sulfur. (a) denotes the 18-electron metal−hydride complex and (b) the 16-electron metal-complex, see the section Models.

conditions. For example, in Ru-catalyzed reactions, which have been studied in most detail, a high enantioselectivity is in particular induced by chiral amino alcohol and *N*-tosylated diamine-based ligands, yielding an enantiomeric excess (ee) of up to 99%.[4,12,22] Excellent reviews on this subject can be found in the literature.[42,43]

To date, it is still a formidable challenge to obtain experimentally direct and accurate insight in the mechanistic pathways of chemical reactions. The most important limitation is the fact that key intermediates often have a very short lifetime. Obviously this holds also for the transition metal catalyzed reactions of the type addressed in the present paper. Computational studies do not suffer from these limitations and provide therefore a valuable complementary approach to study these reactions. To unravel the underlying mechanistic reaction pathway of the metal-catalyzed transfer hydrogenation reactions, a number of computational studies of simplified Ru and Rh model complexes have been performed.[22,44−47] In these studies mainly three types of mechanisms were considered (Scheme 1): (I) concerted transfer of the proton of the amine ligand and the metal-coordinated hydride to the pro-chiral ketone, referred to by Noyori as the metal−ligand bifunctional mechanism,[48] (II) migratory insertion of the pro-chiral ketone into the metal−hydride bond, and (III) direct transfer of the α-hydrogen of the metal−alkoxide complex to the pro-chiral ketone, commonly known as the Meerwein−Ponndorf−Verley reduction.[49,50] For a Ru complex with an amino alcohol ligand Noyori and co-workers,[46] Alonso et al.,[44] and Petra et al.[22] have recently found that the transfer hydrogenation via mechanism I is energetically favorable over the other two mechanisms. For a Rh complex with a primary diamine ligand, Guiral et al.[47] showed that hydrogen transfer prefers mechanism I over a mechanism first proposed by Gladiali et al.[51] which is very similar to II. However, they found that for a Rh complex bearing a tertiary diamine ligand mechanism III is also possible.

To our knowledge computational studies of Ir-catalyzed hydrogen transfer are still absent. However, in view of the good performance of Ir compounds as illustrated by the 92% ee in the reduction of acetophenone using a *N*-(*p*-tolylsulfonyl)-1,2-diphenylethylenediamine ligand,[39] and the 97% ee obtained with amino sulfide ligands in the reduction of aryl−alkyl ketones as reported by Petra et al.,[41] there is an obvious need for further clarification of Ir-catalyzed hydrogen transfer by computational methods.

Here, we report a density functional theory (DFT) study of the Ir-catalyzed transfer hydrogenation of ketones and compare this directly to the well-characterized Ru-catalyzed transfer hydrogenation. Reaction paths for the above-mentioned mechanisms including all important transition states (TSs) are computed. The

(40) Inoue, S.; Nomura, K.; Hashiguchi, S.; Noyori, R.; Izawa, Y. *Chem. Lett.* **1997**, 957−958.
(41) Petra, D. G. I.; Kamer, P. C. J.; Spek, A. L.; Schoemaker, H. E.; van Leeuwen, P. W. N. M. *J. Org. Chem.* **2000**, *65*, 3010−3017.
(42) Zassinovich, G.; Mestroni, G.; Gladiali, S. *Chem. Rev.* **1992**, *92*, 1051−1069.
(43) Noyori, R.; Ohkuma, T. *Angew. Chem., Int. Ed.* **2001**, *40*, 40−73.
(44) Alanso, D. A.; Brandt, P.; Nordin, S. J. M.; Andersson, P. G. *J. Am. Chem. Soc.* **1999**, *121*, 9580−9588.
(45) Guiral, V.; Delbecq, F.; Sautet, P. *Organometallics* **2000**, *19*, 1589−1598.
(46) Yamakawa, M.; Ito, H.; Noyori, R. *J. Am. Chem. Soc.* **2000**, *122*, 1466−1478.
(47) Guiral, V.; Delbecq, F.; Sautet, P. *Organometallics* **2001**, *20*, 2207−2214.
(48) Noyori, R.; Yamakawa, M.; Hashiguchi, S. *J. Org. Chem.* **2001**, *66*, 7931−7944.
(49) Wilds, A. L. *Org. React.* **1944**, *2*, 178−223.
(50) Nishide, K.; Node, M. *Chirality* **2002**, *14*, 759−767.
(51) Gladiali, S.; Pinna, L.; Delogu, G.; Martin, S. D.; Zassinovich, G.; Mestroni, G. *Tetrahedron: Asymmetry* **1990**, *1*, 635−648.

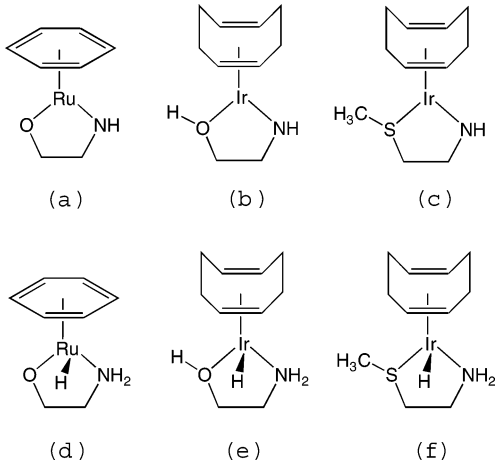

Figure 1. Schematic structures of the 16- (top) and 18-electron (bottom) Ru and Ir complexes.

Scheme 2. Transition Metal Catalyzed Asymmetric Transfer Hydrogenation of Ketones

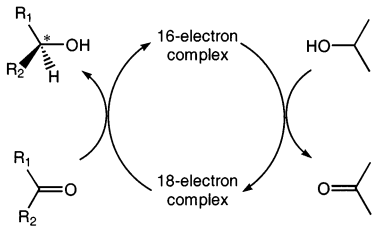

results are mutually compared and put in perspective in a qualitative comparison with experimental results.

Models

Scheme 2 shows the simplified catalytic cycle of asymmetric transfer hydrogenation of ketones.[46,48] A 16-electron complex is generated from a catalyst precursor, typically the corresponding metal halide, using an inorganic base such as KOH, NaOH, or K_2CO_3. In a common experiment 2-propanol acts as both solvent and hydrogen donor. It first reacts with the 16-electron complex to form the 18-electron metal−hydride complex. This in turn reacts with a pro-chiral ketone to form a chiral secondary alcohol. In the case of Ru both the 16- and the 18-electron complex have been isolated and the crystal structure has been elucidated.[8] In the present computational studies we considered a simplified form of a well-performing Ru arene amino alcohol compound,[7] similar to that of Noyori and co-workers,[46] with a stabilizing benzene ligand and an amino ethanol ligand (Figure 1a,d). For the Ir catalyst we considered two simplified models: one with an amino ethanol (Figure 1b,e) ligand and a second with a 2-aminoethylmethyl sulfide ligand (Figure 1c,f), both of them with an additional stabilizing cycloocta-1,5-dienyl (COD) ligand. The chiral analogues of the model amino sulfide ligand yield active catalysts with relatively high ee (80% ee at 82% conversion for the reduction of acetophenone), whereas the Ir compounds with amino alcohol ligands show much lower activity.[41] Experimental work by Petra et al.[41] suggests that in the active catalyst COD is η^4-coordinated to Ir. Crystal structures[37] of an analogous Ir catalyst show also coordination of COD in η^4-mode. Calculations of Bernard et al.[30] that found COD η^4-coordinated in an isoelectronic Rh complex support the suggestion by Petra et al. For the transfer hydrogenation we consider a symmetric model reaction with methanol being the hydrogen donor and formaldehyde representing the ketone.

Table 1. Optimized Bond Lengths (Å) and First Bond Dissociation Energy (FBDE) (kcal/mol) of Ruthenium(II) and Iridium(I) Hexacarbonyl

		r(M−C)	*r*(C−O)	FBDE
$[Ru(CO)_6]^{2+}$	CPMD-BLYP	2.055	1.132	44.8
	ADF-BLYP[a]	2.054	1.129	45.4
$[Ir(CO)_6]^{3+}$	CPMD-BLYP	2.069	1.127	68.2
	ADF-BLYP[a]	2.080	1.122	68.1

[a] Scalar-relativistic corrections are included by way of the zero-order regular approximation (ZORA).[63]

Methods and Validation

We performed DFT-based electronic structure calculations using the BLYP functional, which combines a gradient correction term for the exchange energy as proposed by Becke[52] with a correction for the correlation energy due to Lee, Yang, and Parr.[53] The pseudopotential method is used to restrict the number of electronic states to those of the valence electrons. The interaction with the core electrons is taken into account using semilocal norm-conserving Martins−Troullier pseudopotentials.[54] The Ru and Ir pseudopotentials were of the semicore type including the highest s- and p-shell electrons as valence electrons. They were generated using ionized configurations (Ru^+ and Ir^{2+}) with the electrons treated relativistic in the scalar approximation. The pseudopotential cutoff radii for C, N, O, and H were 1.23, 1.12, 1.10, and 0.50 au, respectively. In case of Ru the radii of the s, p, and d pseudopotentials were 1.10, 1.20, and 1.24 au, respectively. For Ir these values were 1.13, 1.15, and 1.28 au. The electronic states are expanded in a plane-wave basis including waves up to an energy of 70 Ry. Calculations are performed in a cubic periodic box of edge 13.0 Å. Test calculations showed that with this setup structural properties are converged within 0.01 and 0.02 Å for the intra- and intermolecular bonds, respectively. Energies are converged within 0.25 kcal/mol. All calculations are performed with the CPMD package.[55]

We validated the numerical accuracy of our computational approach against benchmark calculations performed with the state-of-the-art atomic orbital based ADF package[56,57] by calculating properties of Ru and Ir hexacarbonyls. Table 1 lists the optimized bond lengths and the first bond dissociation energy (FBDE). The FBDE corresponds to the energy change upon removing one of the carbonyl ligands from the metal hexacarbonyl. To our knowledge no experimental structural data are available. With respect to the bond lengths the agreement between the CPMD and ADF results is excellent, with a maximum deviation of 0.01 Å, but most deviations are within 0.005 Å. Also the FBDEs are in good agreement. This indicates state-of-the-art accuracy of the numerical methods employed in CPMD.

(52) Becke, A. D. *Phys. Rev. A* **1988**, *38*, 3098−3100.
(53) Lee, C. T.; Yang, W. T.; Parr, R. G. *Phys. Rev. B* **1988**, *37*, 785−789.
(54) Troullier, N.; Martins, J. L. *Phys. Rev. B* **1991**, *43*, 1993−2006.
(55) Hutter, J.; Alavi, A.; Deutsch, T.; Bernasconi, M.; Goedecker, S.; Marx, D.; Tuckerman, M.; Parrinello, M. *CPMD*, version 3.4.3; MPI für Festkörperforschung and IBM Zurich Research Laboratory, 1995−1999.
(56) te Velde, G.; Baerends, E. J.; et al. *ADF*, version 2000; Theoretical Chemistry, Vrije Universiteit: Amsterdam, 2000.
(57) Kohn−Sham orbitals are expanded in a triple-ζ basis set augmented with 3d and 4f polarization functions for C and O, 5p and 4f for Ru, and 6p and 5f for Ir. Cores were kept frozen.

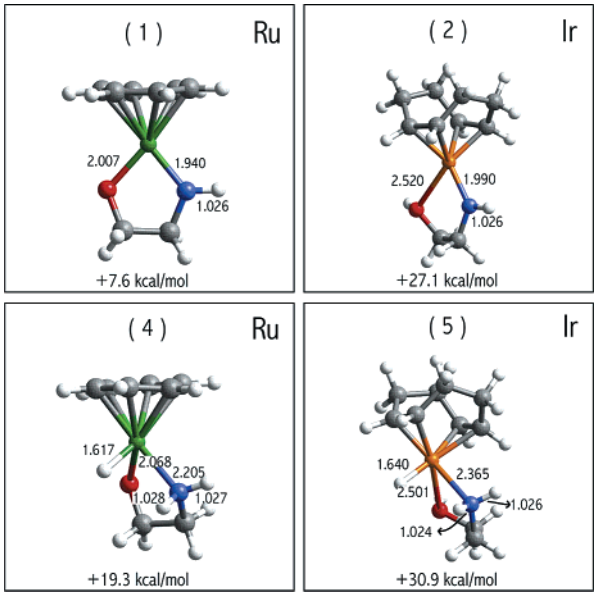

Figure 2. Catalyst structure. Optimized geometries of the 16- and 18-electron Ru and Ir complexes. Energies are relative to the metal−methoxide complexes **21** and **22**.

Zero-point energy (ZPE) corrections are not incorporated in our study. Test calculations performed on the Ru-catalyzed hydrogen transfer via mechanism I showed that the activation barrier for the alcohol oxidation changed from 12.7 to 10.7 kcal/mol if ZPE corrections are included, whereas the barrier for formaldehyde reduction decreased by only 0.3 kcal/mol. Similar ZPE corrections at the B3LYP/6-31G(d,p) level are reported by Noyori and co-workers.[46] While ZPE corrections are clearly not negligible, we will see that for the reactions studied in the present paper the ZPEs are small compared to almost all calculated activation barriers.

Results

Geometrical differences among the Ir complexes with the amino ethanol and 2-aminoethylmethyl sulfide ligands are, for almost all distances, less than 0.1 Å. In the following figures we will therefore show only structures of the complexes with the amino ethanol ligand. (Structures not shown are available via Supporting Information or upon request.) Note that all reported energy values (kcal/mol) are with respect to the energy of the metal−methoxide complex. In the following we will first present results for the bare catalysts, followed by the possible coordinations of the substrates to the catalyst, and finally present results for the different reaction mechanisms.

Catalyst Structure and Substrate Coordination. Figure 2 shows the optimized structures of the 16-electron and the 18-electron complexes, both important intermediates in the catalytic cycle. We observe that for both Ru and Ir the M−N bond is ∼0.3 Å longer for the 18-electron complex compared to the 16-electron complex. This is to be expected since the character of the nitrogen changes from an amide to an amine. The Ru−O bond is also slightly elongated for the 18-electron complex, in contrast to the Ir−O bond, which shows a very small decrease. Overall, it is clear that the ligand coordination is stronger for the 16-electron complex for both the Ru and Ir complex. When comparing the Ru and Ir complexes, the oxygen−metal bond is significantly stronger in the Ru complex. This difference originates from the fact that Ru has a strong, intramolecular-like σ-bond with the oxygen, whereas Ir forms a bond involving one of the oxygen lone pairs that has a more intermolecular nature. Obviously, this difference originates from the different valence configurations of the Ru and Ir atoms, with Ir having one electron more. The metal−hydride bond is ∼1.6 Å for all complexes and similar to that found for the Rh−H bond in the isoelectronic complex $[RhH(NH_3)_2(C_2H_4)_2]$.[30] Apparently this bond length is typical for these metal−hydride complexes and indicates a stable metal−hydride coordination. Note further the reversal of the O−C−C−N torsion angle of the ligand backbone from +53.7° for **4** to −58.1° for **5**. Hence, the mode of ligand coordination is also rather different for Ru compared to Ir.

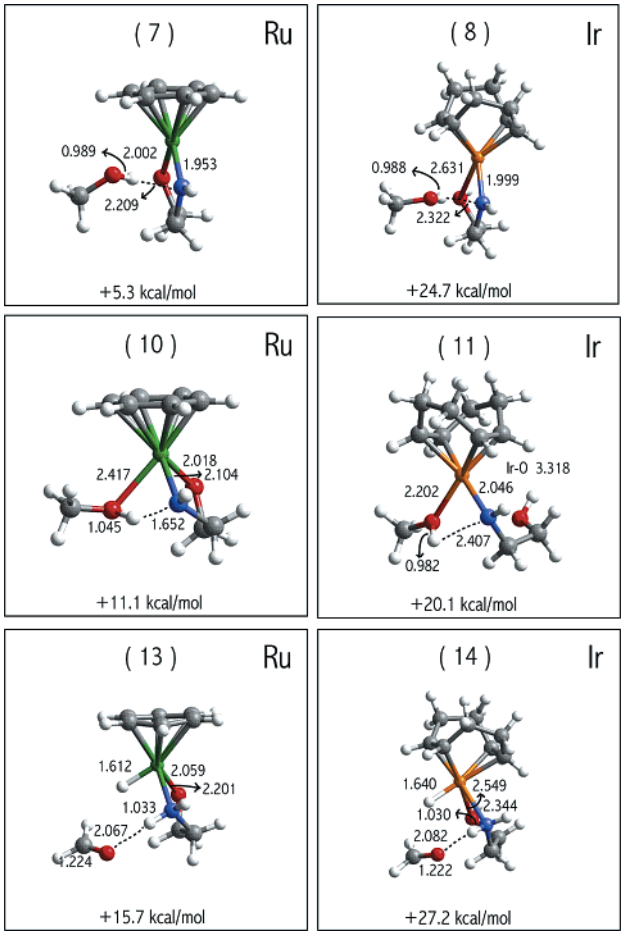

Figure 3. Substrate coordination. Optimized geometries of initial coordination of methanol and formaldehyde to the 16- and 18-electron Ru and Ir complexes. Energies are relative to the metal−methoxide complexes **21** and **22**.

The coordination of methanol and formaldehyde to the 16- and 18-electron Ru and Ir complexes is shown in Figure 3. For the coordination of methanol to the 16-electron complexes we have found two types of stable structures. First, formation of an intermolecular hydrogen bond between the amide nitrogen of the 16-electron complex and the hydroxy group of methanol, **7** and **8**, yields a stabilization of ∼2 kcal/mol. Note also the further elongation of the Ir−O bond by 0.11 Å, while the Ru−O bond length remains the same. The second structure involves a direct coordination to the metal via a lone pair of the methanol oxygen, **10** and **11**. For Ru the oxygen coordination appears relatively weak, with

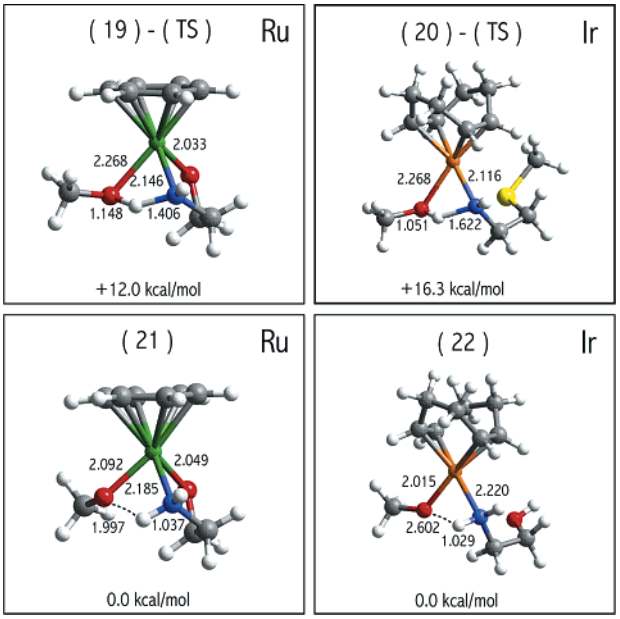

Figure 4. Metal methoxides. Structures of formation of the metal−methoxides. Energies are relative to the metal−methoxide complexes **21** and **23**.

a Ru−O bond length of 2.42 Å, and is accompanied by a short hydrogen bond of 1.65 Å between the hydroxy hydrogen of methanol and the amide nitrogen. In contrast, for Ir the coordination of the methanol oxygen effectively replaces the coordination of the ligand alcohol oxygen that dissociates without any activation barrier and no methanol−amide hydrogen bond is formed. This shows that the ligand in this Ir complex is a clear example of a hemilabile ligand,[58] consistent with the observation for the bare catalysts (supra vide) that the Ir−O bond is weak. Guiral et al.[45] reported a similar decoordination of one of the Rh−N bonds of the diamine ligand in the electronically equivalent Rh complex. Comparing the energies relative to methanol dissociation, we see that the hydrogen-bonded coordination is stable for both the Ru complex and the Ir complexes. The oxygen−metal coordination is even more stable for Ir, but unstable for Ru.

The coordination of formaldehyde to the 18-electron Ru and Ir complexes is very similar to that of the hydrogen-bonded methanol, with the oxygen of formaldehyde hydrogen-bonded to the amine nitrogen, see **13** and **14**. The complexation energy relative to formaldehyde dissociation is ∼4 kcal/mol.

Mechanism of Transfer Hydrogenation

Figure 4 shows the structures of the formation of the metal−methoxide complex. In Figures 5, 6, and 7 we show the optimized structures for the concerted hydrogen-bond, migratory insertion and direct transfer mechanisms, respectively. The overall energy profiles are shown in Figure 8. We did not investigate the direct hydrogen transfer mechanism for the Ru complex. Alonso et al.[44] computed at the B3PW91/6-311+G** level a barrier of 30 kcal/mol and concluded that this mechanism can be excluded.

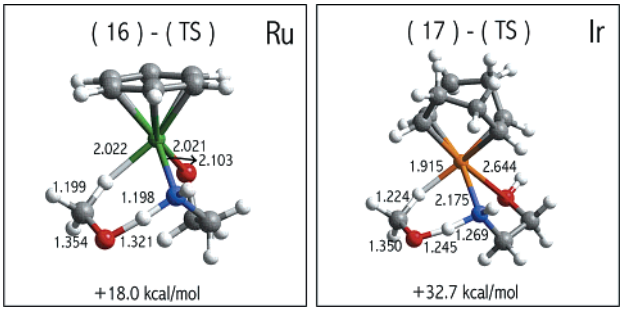

Figure 5. Concerted hydrogen transfer. Transition state structures of the concerted hydrogen transfer (metal−ligand bifunctional mechanism[48]). Energies are relative to the metal−methoxide complexes **21** and **22**.

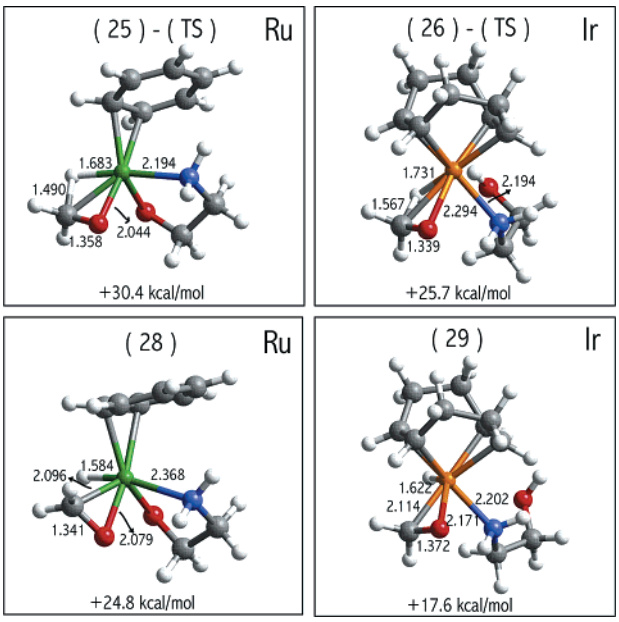

Figure 6. Migratory insertion. Optimized structures of the *β*-elimination/migratory insertion mechanism. Energies are relative to the metal−methoxide complexes **21** and **22**.

Concerted transfer of hydride and proton to the coordinating formaldehyde (Figure 5) is accompanied by a small barrier of 2.3 kcal/mol for the Ru complex: TS **16** is only slightly higher in energy than the formaldehyde-associated complex **13**. If ZPE corrections are included, the barrier is 2.0 kcal/mol. Noyori and coworkers[46] obtained for the same system a barrier of 4.7 kcal/mol (B3LYP/6-311++G(d,p) level including ZPE corrections). This result can be considered consistent with our result, as differences of a few kcal/mol among different density functionals are common. Note that, in general, barriers computed with BLYP are somewhat smaller than those obtained with B3LYP.[59] For the Ir complexes the barriers are also moderate, with a value of 6 kcal/mol for both the amino ethanol (**14** → **17**) and amino sulfide (**15** → **18**) ligands. The reverse reaction, with methanol transferring its hydrogens to the metal complex, yields reaction barriers of 13 kcal/mol (**7** → **16**), 8 kcal/mol (**8** → **17**), and 13 kcal/mol (**9** → **18**), for the Ru complex, Ir amino alcohol, and Ir amino sulfide complexes, respectively.

(58) Braunstein, P.; Naud, F. *Angew. Chem., Int. Ed.* **2001**, *40*, 680−699.

(59) Hamprecht, F. A.; Cohen, A. J.; Tozer, D. J.; Handy, N. C. *J. Chem. Phys.* **1998**, *109*, 6264−6271.

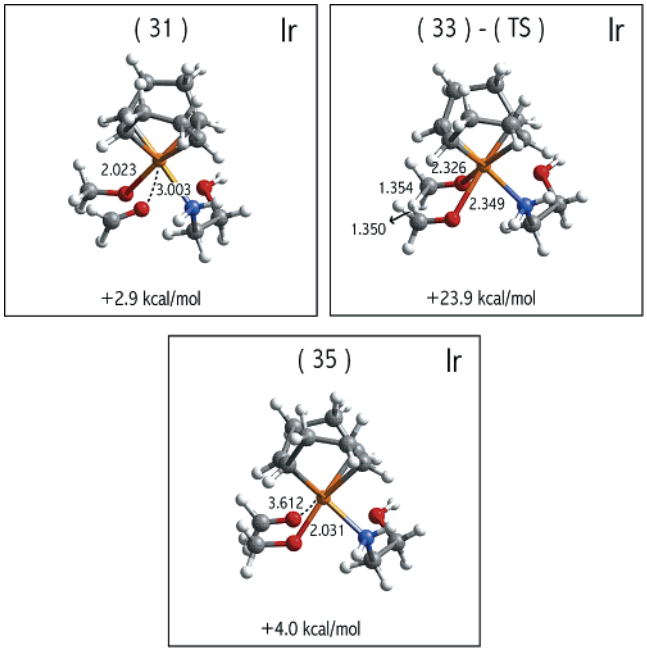

Figure 7. Direct hydrogen transfer. Optimized structures of the Ir-catalyzed direct hydrogen transfer mechanism. Energies are relative to the metal−methoxide complex **22**.

Before describing the migratory insertion and direct transfer mechanisms we first discuss the formation of the metal−methoxide complexes (Figure 4). They are an important intermediate in these mechanisms and obtained via proton transfer from the coordinated methanol to the metal complex. The proton transfer proceeds for the Ru and Ir complexes via negligible barriers, yielding very stable metal−methoxide complexes **21**, **22**, and **23**. Note that especially for Ir the formation of the methoxides is highly exothermic, with energy differences of at least 20 kcal/mol.

For the Ru complex the subsequent β-elimination step (Figure 6) from the Ru methoxide (**21**) to the formaldehyde-coordinated complex **13**, via **24** (configuration **24**, not shown in the figures, constitutes a Ru methoxide complex with an η^2-coordinated benzene), TS **25**, and **28** involves a high-energy barrier of 30 kcal/mol. This is caused by electronic saturation of the metal: in structures **25** and **28** the substrate CO bond is coordinating to the metal, forcing a η^6 to η^2 decoordination of the benzene group. This is also found by others.[44,46] The reverse pathway, i.e., the hydrogenation of the formaldehyde-coordinated Ru complex by migratory insertion, **13** → **21**, shows an energy barrier of 15 kcal/mol.

Also for both Ir complexes we see that the β-elimination step (Figure 6) from the methoxide-coordinated complexes **22** and **23** to the formaldehyde-coordinated complexes **14** and **15** proceeds via high energy barriers, with values of 26 and 30 kcal/mol. Again, for the transition states the coordination of the substrate CO bond induces electronic saturation, giving rise to decoordination of the relatively weakly bound alcohol/sulfide part of the ligand. Also the locally stable complexes **29** and **30**, with the formaldehyde CO π-bond coordinating to the metal, show this decoordination. This explains why, in contrast to the Ru complex, these π-bond-coordinated configurations are stable compared to the formaldehyde hydrogen bonded to the ligand amine group, structures **14** and **15**. The reverse migratory insertion pathway hydrogenating the Ir-coordinated formaldehyde, **29** → **22** and **30** → **23**, shows energy barriers of 8 and 13 kcal/mol for the Ir amino alcohol and Ir amino sulfide complexes, respectively.

In the direct hydrogen transfer mechanism (Figure 7) a formaldehyde coordinates to the Ir methoxide complex, **31** and **32**, and subsequently a methyl hydride is exchanged between the facing methoxide and formaldehyde carbon groups. For both Ir complexes the formaldehyde coordination is accompanied by a slight increase in energy, 1−3 kcal/mol. The subsequent hydride exchange proceeds via an energy barrier of 24 and 19 kcal/mol for the Ir amino alcohol and amino sulfide complexes, respectively. Note that, as for the β-elimination/migratory−insertion transition state, the relatively weakly bound alcohol/sulfide part of the ligand is decoordinated from the Ir atom in the transition state, again due to electronic saturation.

Discussion

From the calculated energy profiles (Figure 8) it is evident that, at least for the gas-phase model systems considered here, the metal−alkoxide complexes comprise an important structure in the catalytic cycle. For the Ru complex the metal−alkoxide complex is stable by at least 5 kcal/mol over any of the other intermediates along the reaction paths. For the Ir complexes this energy difference is far more pronounced: 17 and 16 kcal/mol for the amino alcohol- and amino sulfide-coordinated complexes, respectively. Noyori and co-workers refer to these stable complexes as "reservoirs" or "sinks".[46] Halpern already pointed out in the early 1980s that such reservoir species may play an important role in stabilizing catalytic systems.[60]

The energy profiles of the concerted hydrogen transfer and migratory insertion/β-elimination mechanism for the Ru complexes (Figure 8, upper profile) provides a picture that is fully consistent with the B3LYP and MP4 results of Noyori and co-workers.[46] It is also in qualitative agreement with computational studies of very similar model systems.[22,44] Comparison of the energy profiles shows that the concerted hydrogen transfer pathway has the lowest transition state energy, with a local barrier of 2 kcal/mol for the hydrogenation of formaldehyde (**13** → **16**) and 13 kcal/mol for the dehydrogenation of methanol (**7** → **16**). A direct consequence is that the stable metal−methoxide complex, intermediate in the migratory insertion/β-elimination pathway, is on a nonproductive route and will give rise to a reservoir of inactive catalysts. Note that the methanol decoordination of the metal−methoxide intermediate involves a reaction barrier of 12 kcal/mol (**21** → **19**), which is comparable to the dehydrogenation barrier (**7** → **16**), and therefore of importance for the overall kinetics of the catalytic cycle. The calculations strongly suggest that the methanol dehydrogenation is the rate-limiting step, whereas formaldehyde hydrogenation proceeds relatively easily. Analysis of an experimental study of a Ru complex with a proper diamine derivative ligand arrived at the same conclusion.[8]

The energy profiles for the Ir complexes (Figure 8, middle and lower profile) provide a different picture.

(60) Halpern, J. *Inorg. Chim. Acta* **1981**, *50*, 11−19.

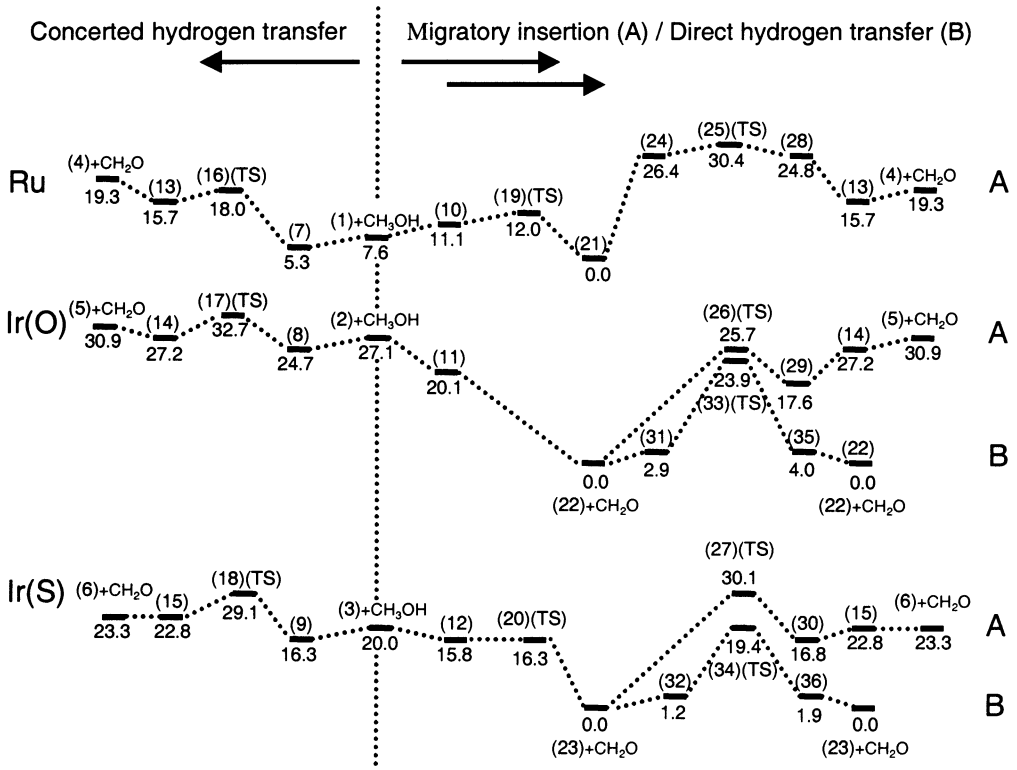

Figure 8. Energy profiles for the concerted hydrogen transfer (left), migratory insertion (right, A), and direct hydrogen transfer (right, B). Ir(O) denotes the Ir catalyst with an amino ethanol ligand and Ir(S) that with 2-aminoethylmethyl sulfide ligand. The energy profile for Ru-catalyzed direct hydrogen transfer is not calculated, see text. Note that the energy profiles for the direct hydrogen transfer involve the metal complex, one methanol, and one formaldehyde. Energies in kcal/mol (without ZPE corrections) are relative to the metal−methoxide complexes **21**−**23**.

Comparison of the energy profiles for the amino alcohol-coordinated Ir complex shows that the β-elimination (**22** → **26**) and direct hydrogen transfer (**22** → **33**) are competing mechanisms, with transition state energies at least 6 kcal/mol lower than that of the concerted hydrogen transfer route. However, in the catalytic cycle of the migratory insertion/β-elimination mechanism the highest energy intermediate state is the 18-electron Ir complex **5**, whereas in the direct hydrogen transfer mechanism this intermediate does not appear, and the highest energy intermediate state, i.e., the 16-electron Ir complex **2**, is 4 kcal/mol lower. Hence, the calculations suggest that the direct hydrogen transfer mechanism is preferred. For the amino sulfide-coordinated Ir complex the direct hydrogen transfer mechanism (**23** → **34**) has by far the lowest transition state energy, with a barrier for hydride exchange (**23** → **34** → **23**) of 19 kcal/mol. Hence, also for the amino sulfide-coordinated Ir complex our calculations suggest that the 18-electron Ir complex does not participate actively in the catalytic cycle. For both Ir complexes the methanol decoordination energy of the Ir methoxide complexes **22** and **23**, with values of 27 and 20 kcal/mol, respectively, is significant and comparable to the energy barrier for the direct hydrogen transfer. They are therefore, as in the Ru system, important for the kinetics of the full catalytic cycle. For the amino alcohol-coordinated complex the energy difference between lowest and highest energy intermediate along the reaction path (27 kcal/mol) is significantly higher than that of the amino sulfide-coordinated complex (20 kcal/mol). This indicates a lower activity of the former complex, consistent with experimental observations.[41]

The mechanisms for Ru- and Ir-catalyzed transfer hydrogenation suggested by our calculations are consistent with the experimental observation that for Ir complexes the enantioselective distribution is dominated by the choice of the hydrogen source,[41] whereas for Ru complexes the choice of the hydrogen source does not effect the stereochemical outcome.[12]

Comparing the energy profiles of the Ru complex and Ir complexes may give an indication why the reaction pathways are different for both complexes. Taking the isolated methanol and 16-electron metal complexes, structures **1**, **2**, and **3**, as reference, we see that the transition state energies for the concerted hydrogen transfer mechanism show a small spread. In contrast, for the transition states for the migratory insertion or direct hydrogen transfer mechanism the energy difference between the Ru and Ir transition states is significant, with the Ir transition state energies more than 20 kcal/mol lower. This relative difference in transition state energies can be qualitatively understood from the structure of the transition states **25**, **26**, **27**, **33**, and **34**. Both the migratory insertion and direct hydrogen transfer mechanism require a transition state with a high coordination of the metal. To prevent electronic oversaturation, one of the stabilizing ligands has to change coordination. For the Ru complex this is achieved by η^6 to η^2 partial decoordination of the strongly bound benzene ligand, whereas for the Ir complexes the alcohol/sulfide part of the hemilabile amino alcohol/amino sulfide ligand decoordinates. The latter is not possible in the Ru complex that has a strongly bound amino alcohol group. The coordination change of the strongly bound benzene ring is far more destabilizing

than the decoordination of the weakly bound alcohol/sulfide group, giving rise to the observed difference in the transition state energies of more than 20 kcal/mol.

For the Ir compounds it is not clear how chiral induction is achieved when the amino alcohol/amino sulfide ligand is partially de coordinated. However, Noyori and co-workers[64] showed for the ruthenium(II)-catalyzed asymmetric hydrogen transfer that a large part of the chiral induction is *electronic* and not *steric* in nature, caused by the attractive CH/π interaction between the η^6-arene and the aromatic substituent in carbonyl substrates. A similar effect can also be envisaged for the iridium(I)-catalyzed transfer since experiments showed that the catalytic performance is far superior for aromatic ketones compared to dialkyl ketones.[41,61] Further computational studies including pro-chiral substrates should reveal the origin of enantioselection for the iridium(I)-catalyzed transfer hydrogenation.

Another important aspect is the role of the solvent, in particular when they strongly interact with the catalyst and the substrates as in the present case, where commonly used solvents are 2-propanol and formic acid. Alonso et al.[44] showed that incorporating electrostatic effects by a simple polarized continuum model (PCM) already has a substantial effect on barrier heights. Moreover, these type of solvents may form strong hydrogen bonds with both the substrate and catalyst. This may also have a large impact on the reactivity of the catalyst. For example, Burk et al.[62] showed that the Rh-catalyzed hydrogenation of enol esters in methanol gave 100% conversion, while benzene as solvent inhibited the reaction completely. The influence of the solvent can be particularly important for hemilabile ligands where there is no rigidly defined catalyst structure, and a solvent molecule can more easily coordinate to the metal or ligand.

Summary

We have performed a DFT-BLYP-based computational study to compare model systems for transfer hydrogenation reactions among alcohols and ketones catalyzed by Ru amino alcohol, Ir amino alcohol, and Ir amino sulfide complexes. In this comparison we considered three reaction mechanisms: (1) concerted hydrogen transfer, also known as the metal−ligand bifunctional mechanism,[46] (2) migratory insertion, and (3) direct hydrogen transfer. Our results for the Ru complex system are fully consistent with the results of Noyori and co-workers,[46] who studied the same model system using DFT-B3LYP and MP4 computational methods. The calculations suggest that the reaction mechanism for the Ru- and Ir-catalyzed reactions are fundamentally different. For the Ru complex the reaction proceeds via concerted hydrogen transfer, whereas for both the Ir amino alcohol and Ir amino sulfide complexes the reaction proceeds via direct hydrogen transfer between simultaneously coordinated ketone and alcohol. This is consistent with experimental data on the dependence of the enantioselective distribution on the hydrogen source. Comparing the results for the Ir amino alcohol and Ir amino sulfide complexes we found our results to be consistent with the experimental data, with the Ir amino alcohol energy profile showing a significantly higher reaction barrier.

For both the Ru and Ir complexes the metal−alkoxide complex plays an important role. In all cases they constitute the most stable complex. In the Ru-catalyzed reaction it is not an intermediate of the reaction mechanism and therefore gives rise to a reservoir of inactive catalysts. In contrast, for the Ir-catalyzed reaction it is an intermediate along the reaction path.

The calculations suggest that the distinction between reaction mechanism for Ru and Ir complexes can be attributed to differences in the nature of the binding of the ligands. The direct hydrogen transfer mechanism, as well as the migratory insertion mechanism, requires partial decoordination of the ligands. For the Ru complex this is achieved by a η^6 to η^2 partial decoordination of the strongly bound benzene ligand, whereas for the Ir complexes the alcohol/sulfide part of the hemilabile amino alcohol/amino sulfide ligand decoordinates relatively easily. Consequently, the transition state of the Ru complex is far more destabilized than the Ir transition state.

Finally we should mention that computational studies such as presented here, although at the limit of present day capabilities, are still open for significant improvement. The variation in calculated energy profiles among different computational methods, e.g., DFT versus MP4,[46] indicates that the underlying electronic structure calculation has an inaccuracy that is not negligible. This should be improved in order to be able to do precise quantitative predictions. Second, the role of the solvent, neglected in the present study as well as in most related studies reported in the literature, is expected to be significant. This holds in particular for metal-catalyzed transfer hydrogenation in alcohol solutions, where there are relatively large changes in solvation energies due to strong hydrogen bonding among substrate, catalyst, and solvent. This implies that a truly realistic description requires incorporation of solvent molecules.

Acknowledgment. J.-W.H. acknowledges NWO-CW (Nederlandse Organisatie voor Wetenschappelijk Onderzoek, Chemische Wetenschappen) through PIONIER. E.J.M. acknowledges the Royal Netherlands Academy of Art and Sciences for financial support. We acknowledge support from the Stichting Nationale Computerfaciliteiten (NCF) and the Nederlandse Organisatie voor Wetenschappelijk Onderzoek (NWO) for the use of supercomputer facilities.

Supporting Information Available: Cartesian coordinates of the optimized structures **1**−**36** (PDF) are available free of charge via the Internet at http://pubs.acs.org.

OM030104T

(61) Petra, D. G. I. Asymmetric Transfer Hydrogenation of Ketones. Thesis, University of Amsterdam, Institute of Molecular Chemistry, 1999.
(62) Burk, M. J.; Kalberg, C. S.; Pizzano, A. *J. Am. Chem. Soc.* **1998**, *120*, 4345−4353.
(63) van Lenthe, E.; Ehlers, A.; Baerends, E. J. *J. Chem. Phys.* **1999**, *110*, 8943−8953.
(64) Yamakawa, M.; Yamada, I.; Noyori, R. *Angew. Chem., Int. Ed.* **2001**, *40*, 2818−2821.